CRYSTAL GROWTH & DESIGN

pubs.acs.org/crystal

Article

Side Chain Induced Self-Assembly and Selective Catalytic Oxidation Activity of Copper(I)−Copper(II)-N_4 Complexes

Yun-Long Hou,* Yun-Lei Peng, Yingxue Diao, Jie Liu, Lizhuang Chen,* and Dan Li*

Cite This: *Cryst. Growth Des.* 2020, 20, 1237−1241

Read Online

ACCESS | Metrics & More | Article Recommendations | Supporting Information

ABSTRACT: Crystalline coordination architectures with coordinatively unsaturated metal sites are of great importance for their attractive properties. Tunable side chains of the 4-formylimidazole here were employed for directing the subcomponent self-assembly of $(Cu^{II}N_4)_2(Cu^{I}I)_2$ (**1**), $\{(Cu^{II}N_4)(Cu^{I}I)_2\}_n$ (**2**), and $\{L(Cu^{I}I)_2\}_n$ (**3**) under the same solvothermal conditions, giving the structural diversity. The unique square-planar $Cu^{II}/Ni^{II}N_4$ units with open metal sites can not only be in situ embedded in **1** and **2**, but also be successfully immobilized in $\{(Ni^{II}N_4)_2(Cu^{I}CN)_9\}_n$ (**4**) and $\{(Cu^{II}N_4)_2(Cu^{I}CN)_9\}_n$ (**5**), through the metalloligand strategy. Enzyme-like substrate-specific activity was observed by employing **5** as a heterogeneous catalyst, which exhibits increased activity and high selectivity toward the catalytic oxidation of 1-phenylethyl alcohol derivatives. This work presents two promising methodologies for the introduction of controllable open metal sites in versatile crystalline coordination complexes and their application in the substrate-selective catalytic oxidation reaction.

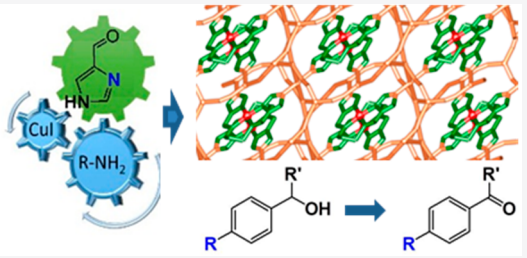

1. INTRODUCTION

It has long been of interest to worldwide researchers to prepare metalloporphyrins and salen-based derivatives, due to their square-planar 4-coordinated units, accessible functionalization and tunable structures, etc.[1−4] Recently, crystalline metal coordination compounds[5−7] such as metallacycles,[3,8,9] rotaxanes,[10] cages,[11] metal−organic frameworks (MOFs), and one-/two-dimensional (1D/2D) coordination polymers (CPs) can be built with such square-planar 4-coordinated metalloligand,[12−16] featuring breathtaking properties such as catalysis,[14,15] separation,[11,13] photoluminescence,[9] and light-harvesting materials.[16,17] It is highly worthwhile to introduce the square-planar 4-coordinated units into the self-assembly of well-defined crystalline structures.

Several methodologies have been developed for the integration of metallosalen/metalloporphyrin struts with MOFs, including noncovalent encapsulation,[18] metalloligand self-assembly,[7,12−15] and postsynthetic modification/exchange,[14] in the research groups of Hupp,[6,19] Goldberg,[20] Zhou,[21] Ma,[16] Cui,[11,13] and others.[22,23] Our group has prepared several copper(I)-based CPs with catalytically active metallosalen moieties, showing promising photocatalytic and transitional metal catalytic activities.[24−26] However, the rational design of metalloligands and synthesis of heterogeneous catalytic materials with predesigned structural moieties and tunable catalytic activities remain a great challenge. The successful practice of crystalline materials with square-planar 4-coordinated units is limited due to the solubility of metalloligand precursors, the large-scale preparation, and rigid reaction conditions.

Side chain functionalization is very powerful for the controllable synthesis and improved properties of various materials during organic and solid-state synthesis.[27−47] Here, we succeed in building square-planar metalloligands and tetrahedral Cu^{I}-based subunits into four complexes, ranging from dimer, 1D chain, and 2D layer coordination structures, $(Cu^{II}N_4)_2(Cu^{I}I)_2$ (**1**), $\{L(Cu^{I}I)_2\}_n$ (**3**), $\{(Ni^{II}N_4)_2(Cu^{I}CN)_9\}_n$ (**4**), and $\{(Cu^{II}N_4)_2(Cu^{I}CN)_9\}_n$ (**5**), through the tunable side chain functionalization of the imidazole precursors. The $Cu^{II}/Ni^{II}N_4$ unit represents the square-planar metalloligand with one 4-coordinated Cu^{II}/Ni^{II} ion and the chelating nitrogen ligand. The enzyme-like substrate selectivity was observed by employing **5** as a heterogeneous catalyst, which exhibits increased activity and high selectivity toward 1-phenylethyl alcohol derivatives. These complexes have been formulated and characterized on the basis of elemental analyses, IR spectroscopy, thermogravimetric (TG), and single-crystal X-ray diffraction analyses (see the Supporting Information, for experimental details).

2. EXPERIMENTAL SECTION

See the Supporting Information for detailed material synthetic procedures, characterization, and other information.

Received: November 7, 2019
Revised: January 3, 2020
Published: January 6, 2020

https://dx.doi.org/10.1021/acs.cgd.9b01499
Cryst. Growth Des. 2020, 20, 1237−1241

3. RESULTS AND DISCUSSION

3.1. Side Chain Induced Self-Assembly. Complexes **1**, **2**, and **3** can be readily prepared via solvothermal three-component self-assembly of oxalyl dihydrazide, CuI, and 4-formylimidazole with or without substituents, in an ethanol/water mixture at 120 °C for 3 days (see the Supporting Information for details). In the absence of side chains on the imidazole ring, CP **2** presents a one-dimensional zigzag chain with square-planar 4-coordinated Cu^{II} atoms,[26] while the replacement of 4-formylimidazole with 5-methyl-4-formylimidazole and 2-ethyl-4-methyl-5-formylimidazole under the same reaction conditions gave gray block-like **1** and red block-like CP **3**, respectively. X-ray single-crystal diffraction analyses revealed that structures of complexes **1**, **2**, and **3** range from simple dimer to one-dimensional chain as shown in Figure 1.

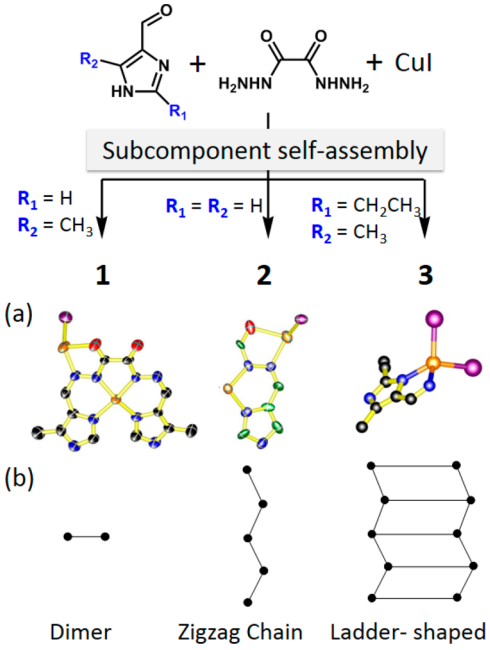

Figure 1. Syntheses of **1**, **2**, and **3** via three-component self-assembly. (a) Asymmetric units; (b) simplified topologies. (a, color codes: Cu, gold; C, black; N, blue; I, purple.).

Among them, mix-valence complex **1** (Tables S1 and S2, in the Supporting Information) contains the twisted square-planar 4-coordinated Cu^{II} atom and the tetrahedral Cu^{I} atom in the asymmetric unit (Figure 1a). In the asymmetric unit of complex **3** (Figure 1a, Tables S1 and S3), the copper(I) atom adopts tetrahedral 4-coordination configuration, which is coordinated to the chelating ligand (**L**) to form a ladder-shaped one-dimensional chain.

In both structures of complexes **1** and **2**, $Cu^{II}N_4$ subunits exist with the coordinatively unsaturated metal sites (CUSs) through synergistic self-assembly of starting subcomponents (Figures 2a and S1). Interestingly, the insertion of 2-ethyl group on the imidazole ring leads to the tetrahedral Cu^{I}-dominated coordination geometry in complex **3** and induces the decarboxylation and imine formation to give the ligand **L** (Figure 2b,c). Considering the steric effect of two adjacent imidazole rings, bulky alkyl groups undoubtedly hinder the driven force to achieve the $Cu^{II}N_4$ planar model. Hence, side-chain functionalization of the starting components provides a meaningful way for directing coordination-driven self-assembly and construction of target compounds.

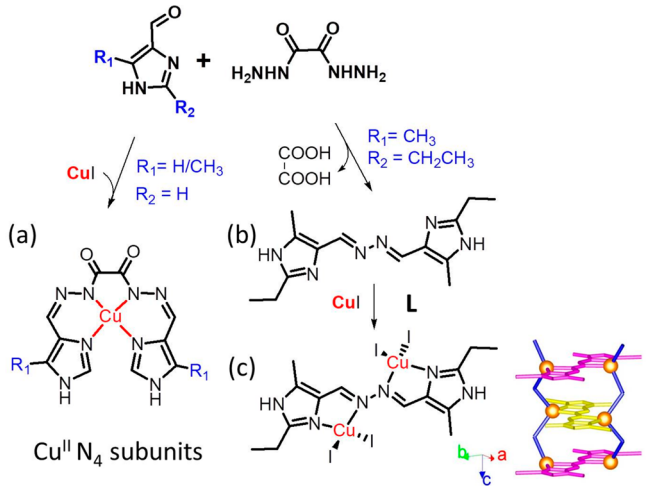

Figure 2. (a) In situ formation of $Cu^{II}N_4$ subunits in complexes **1** and **2**. (b) In situ synthesis of ligand **L** via the imine formation and decarboxylation in complex **3**. (c) The tetrahedral Cu^{I} coordination model and representive 1D ladder-shaped chain of **3**.

3.2. Metalloligand Self-Assembly. As an effort to explore other effective methodologies to immobilize the square-planar 4-coordinated units in the crystalline materials, we have also turned to the metalloligand strategy.[7,25,48−51] Unlike the subcomponent self-assembly as mentioned above, heterometallic 2D CPs **4** and **5** were successfully obtained by the reaction of Cu^{II}/Ni^{II} N_4 precursors and CuCN in a molar ratio of 2:9 in a DMF/acetonitrile mixture (v/v, 3:1) at 120 °C for 3 days (Figure 3a, see also the Supporting Information for details). X-ray diffraction analyses revealed that $\{(Ni^{II}N_4)_2(Cu^{I}CN)_9\}_n$ (**4**) and $\{(Cu^{II}N_4)_2(Cu^{I}CN)_9\}_n$ (**5**) are isostructural to each other, crystallized in the triclinic $P\bar{1}$ space group (Tables S1, S4, and S5). The asymmetric unit of **5** contains one deprotonated $Cu^{II}N_4$ metalloligand connected by two separate Cu^{I} atoms of the linear CuCN chain. The two Cu^{I} atoms adopt 2-coordinated linear geometry and 3-coordinated triangular geometry, respectively (Figure 3b). The $Cu^{II}N_4$ moieties are linked by infinite $[CuCN]_n$ chains to form a two-dimensional layer along the *b*-axis (Figures 3c and S2). Both structures of **4** and **5** (Tables S4 and S5) feature weak $Cu^{I}\cdots Cu^{I}$ interactions between adjacent Cu^{I} atoms of $[CuCN]_n$ chains, which was used to encapsulate $Cu^{II}/Ni^{II}N_4$ units.

Complexes **1**−**5** were found to be highly stable in air and water based on powder X-ray diffraction (PXRD) experiments and insoluble in DMF, ethanol, and acetonitrile (<0.5 mg/mL). The thermal stabilities rise from 300 °C (**1**), 300 °C (**4** and **5**) to 330 °C (**3**) based on thermogravimetric analyses (Figures S3−S6). Phase purity of the bulk samples was established by comparison of their observed and simulated PXRD patterns (Figures S7−S10).

3.3. Selective Catalytic Oxidation of Aromatic Alcohols. The transitional metal catalytic properties of $Cu^{II}N_4$ subunit were investigated through a model reaction of the catalytic oxidation of aromatic alcohols to the corresponding aldehydes or ketones. The reaction was conducted using 3.0 mmol % of CP **5** as the catalyst and 1.5 equiv of TBHP as the oxidant with acetonitrile as the solvent at 20 °C under atmospheric pressure (see Supporting Informa-

https://dx.doi.org/10.1021/acs.cgd.9b01499
Cryst. Growth Des. 2020, 20, 1237−1241

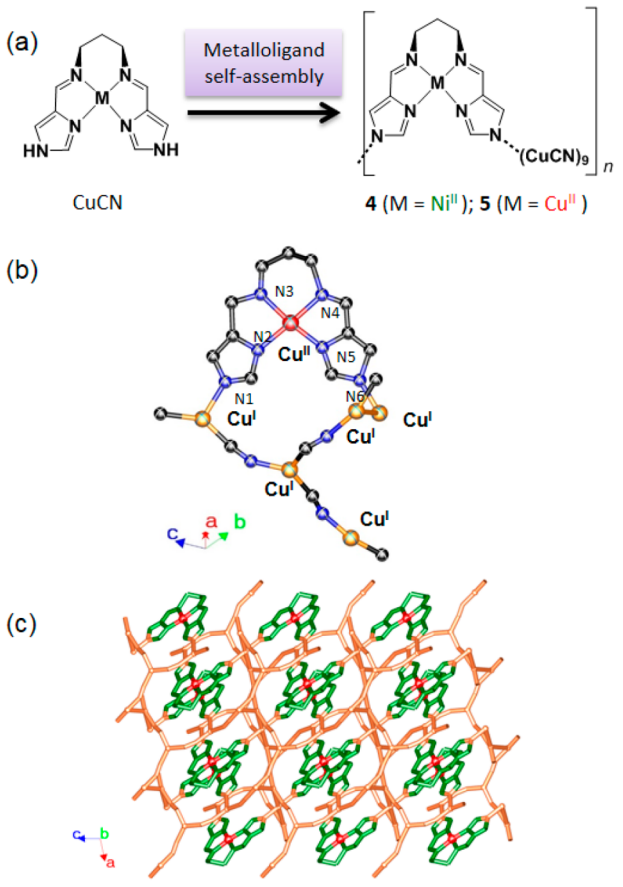

Figure 3. (a) Syntheses of **4** and **5** via metalloligand precursors. (b) The copper(II)-N_4 asymmetric unit. Color codes: Cu^I, gold; Cu^{II}, red; C, black; N, blue. (c) The representative 2D layer of complex **5** along the *b*-axis. The hydrogen atoms were omitted for clarity.

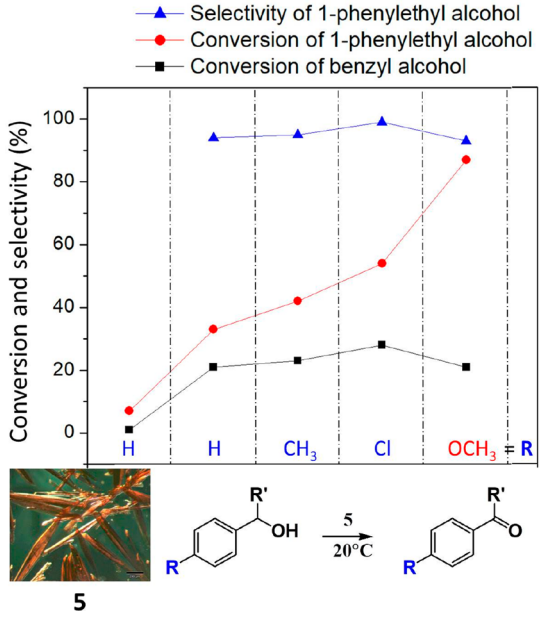

Figure 4. Illustration of the substrate-specific catalytic oxidation behavior in the conversion of four 1-phenylethyl alcohol derivatives (R = H, CH_3, Cl, and OCH_3) to the corresponding ketones by employing bulky crystalline complex **5** (see the photo) as a solid catalyst. Five points represent (red and black, from left to right) conversations of the blank experiment and substrates without or with substituted groups of methyl, chloro, methoxyl. Four blue points represent product selectivities of each substrate. The reaction was performed at 293 K.

tion for details). Table S6 lists the substrate (aromatic alcohols) conversion, the product selectivity (moles of aldehydes/ketones per mole of total products), and turnover frequency (TOF, moles of products per mole of catalysts per hour) of **5**. For the oxidation of 1-phenylethyl alcohol and benzyl alcohol, only 7% and <1% conversion was observed in blank experiments respectively (Table S6, entries 1 and 6). In the presence of catalyst **5**, 33% conversion and 94% selectivity were observed for 1-phenylethyl alcohol. Although this conversion was limited by the bulky crystal with accessible catalytic sites only located on the solid surface (see Figure 4), good catalytic efficiency can be achieved for the 1-phenylethyl alcohol with substituted groups of methyl, chloro, and methoxyl, which show high selectivities (93−99%) and an increased conversions of 42%, 54%, and 87%, respectively (see Figure 4). However, this substrate-selective catalytic phenomenon was not observed for that of benzyl alcohol, which gave a low conversion of about 20%. Hence, it should be pointed out that both 1-position and R groups of 1-phenylethyl alcohol contributed to this catalytic efficiency. It is interesting that for us to further investigate the supramolecular interaction mechanism between side chains of 1-phenylethyl alcohol and the open metal sites located on the bulky crystalline layered structure.

To examine the heterogeneous catalytic nature of crystalline coordination solid,[52−54] the chemical stability and catalytic recyclability of **5** was examined. After three cycles of repeated reactions, the conversions and selectivities of benzyl alcohol to benzaldehyde were maintained (Table S6, entries 7−9). Atomic absorption spectroscopy (AAS) measurement was conducted to show less than 0.1% copper metal leached out in the solution. The powder X-ray diffraction (PXRD) analysis of the solid residues recovered after three cycles illustrates a similar pattern as that of the pristine solids (Figure S10). The above results confirm that CP **5** is heterogeneous catalytic materials, which can be recycled under mild conditions (e.g., low temperature, short time, and suitable oxidant).

4. CONCLUSION

In summary, we have constructed copper(I)-based complexes with planar copper(II)/nickel(II) N_4 metalloligands through both one-pot self-assembly and metalloligand strategies. Differences in side chains of the synthetic precursors were managed to tune the coordination-driven self-assembly, targeting versatile architectures under the same reaction condition. Furthermore, when the crystalline bulky material behaved as a heterogeneous catalyst in the oxidation of aromatic alcohols, substrate-specific and enhanced catalytic efficiency was achieved by **5**, indicating the enzyme-like weak interaction between the catalytic sites and the substrate. Considering the significance of dynamic catalytically active species in polymeric materials, side chain modification and rational design of active sites are a promising way for controlling the self-assembly behavior and catalytic transition state.

https://dx.doi.org/10.1021/acs.cgd.9b01499
Cryst. Growth Des. 2020, 20, 1237−1241

■ ASSOCIATED CONTENT

Supporting Information

The Supporting Information is available free of charge at https://pubs.acs.org/doi/10.1021/acs.cgd.9b01499.

Additional physical measurements and structural analyses (PDF)

Accession Codes

CCDC 1956573−1956576 contain the supplementary crystallographic data for this paper. These data can be obtained free of charge via www.ccdc.cam.ac.uk/data_request/cif, or by emailing data_request@ccdc.cam.ac.uk, or by contacting The Cambridge Crystallographic Data Centre, 12 Union Road, Cambridge CB2 1EZ, UK; fax: +44 1223 336033.

■ AUTHOR INFORMATION

Corresponding Authors

Yun-Long Hou − *Jiangsu University of Science and Technology, Zhenjiang, China;* orcid.org/0000-0003-3828-5569; Email: ylhou8@just.edu.cn

Lizhuang Chen − *Jiangsu University of Science and Technology, Zhenjiang, China;* orcid.org/0000-0001-8582-599X; Email: clz1977@sina.com

Dan Li − *Jinan University, Guangzhou, China;* orcid.org/0000-0002-4936-4599; Email: danli@jnu.edu.cn

Other Authors

Yun-Lei Peng − *Jinan University, Guangzhou, China*

Yingxue Diao − *City University of Hong Kong, Kowloon, Hong Kong, China*

Jie Liu − *Suzhou University of Science and Technology, Suzhou, China;* orcid.org/0000-0003-3179-4643

Complete contact information is available at: https://pubs.acs.org/10.1021/acs.cgd.9b01499

Notes

The authors declare no competing financial interest.

■ ACKNOWLEDGMENTS

We acknowledge the National Natural Science Foundation of China (Nos. 21731002, 21975104, 21671084, and 21702143); Natural Science Foundation of Jiangsu Province (Nos. BK20131244, BK20170377); Six talent peaks project in Jiangsu Province (No. 2014-XCL-008); the Qing Lan Project of Jiangsu Province; the Innovation Program of Graduate Students in Jiangsu Province (No. KYLX16-0508); a Project Funded by the Priority Academic Program Development of Jiangsu Higher Education Institution; Innovation Program for Graduate Student from Jiangsu University of Science and Technology (No. YCX15S-19) and the Foundation of Jiangsu Educational Committee (No. 16KJB430011).

■ REFERENCES

(1) Cozzi, P. G. Metal-salen Schiff base complexes in catalysis: practical aspects. *Chem. Soc. Rev.* **2004**, *33*, 410−421.

(2) Ma, L. Q.; Falkowski, J. M.; Abney, C.; Lin, W. B. A series of isoreticular chiral metal-organic frameworks as a tunable platform for asymmetric catalysis. *Nat. Chem.* **2010**, *2*, 838−846.

(3) Beletskaya, I.; Tyurin, V. S.; Tsivadze, A. Y.; Guilard, R.; Stern, C. Supramolecular chemistry of metalloporphyrins. *Chem. Rev.* **2009**, *109*, 1659−1713.

(4) Drain, C. M.; Varotto, A.; Radivojevic, I. Self-organized porphyrinic materials. *Chem. Rev.* **2009**, *109*, 1630−1658.

(5) Crane, A. K.; MacLachlan, M. J. Portraits of porosity: porous structures based on metal salen complexes. *Eur. J. Inorg. Chem.* **2012**, *2012*, 17−30.

(6) Morris, G. A.; Nguyen, S. T.; Hupp, J. T. Enhanced activity of enantio selective (salen)Mn(III) epoxidation catalysts through supramolecular complexation. *J. Mol. Catal. A: Chem.* **2001**, *174*, 15−20.

(7) Lu, W. G.; Wei, Z. W.; Gu, Z. Y.; Liu, T. F.; Park, J.; Park, J.; Tian, J.; Zhang, M. W.; Zhang, Q.; Gentle, T., III; Bosch, M.; Zhou, H. C. Tuning the structure and function of metal-organic frameworks via linker design. *Chem. Soc. Rev.* **2014**, *43*, 5561−5593.

(8) Sun, S. S.; Stern, C. L.; Nguyen, S. T.; Hupp, J. T. Directed assembly of transition-metal-coordinated molecular loops and squares from salen-type components. Examples of metalation-controlled structural conversion. *J. Am. Chem. Soc.* **2004**, *126*, 6314−6326.

(9) Dong, J. Q.; Tan, C. X.; Zhang, K.; Liu, Y.; Low, P. J.; Jiang, J. W.; Cui, Y. Chiral NH-controlled supramolecular metallacycles. *J. Am. Chem. Soc.* **2017**, *139*, 1554−1564.

(10) Narita, M.; Yoon, I.; Aoyagi, M.; Goto, M.; Shimizu, T.; Asakawa, M. Transition metal(II)-salen and -salophen macrocyclic complexes for rotaxane formation: syntheses and crystal structures. *Eur. J. Inorg. Chem.* **2007**, *2007*, 4229−4237.

(11) Xuan, W. M.; Zhang, M. N.; Liu, Y.; Chen, Z. J.; Cui, Y. A chiral quadruple-stranded helicate cage for enantioselective recognition and separation. *J. Am. Chem. Soc.* **2012**, *134*, 6904−6907.

(12) Cho, S. H.; Ma, B. Q.; Nguyen, S. T.; Hupp, J. T.; Albrecht-Schmitt, T. E. A metal-organic framework material that functions as an enantioselective catalyst for olefin epoxidation. *Chem. Commun.* **2006**, 2563−2565.

(13) Li, G.; Zhu, C. F.; Xi, X. B.; Cui, Y. Selective binding and removal of organic molecules in a flexible polymeric material with stretchable metallosalen chains. *Chem. Commun.* **2009**, 2118−2120.

(14) Shultz, A. M.; Sarjeant, A. A.; Farha, O. K.; Hupp, J. T.; Nguyen, S. T. Post-synthesis modification of a metal-organic framework to form metallosalen-containing MOF materials. *J. Am. Chem. Soc.* **2011**, *133*, 13252−13255.

(15) Xi, W. Q.; Liu, Y.; Xia, Q. C.; Li, Z. J.; Cui, Y. Direct and post-synthesis incorporation of chiral metallosalen catalysts into metal-organic frameworks for asymmetric organic transformations. *Chem. - Eur. J.* **2015**, *21*, 12581−12585.

(16) Gao, W. Y.; Chrzanowski, M.; Ma, S. Q. Metal-metalloporphyrin frameworks: a resurging class of functional materials. *Chem. Soc. Rev.* **2014**, *43*, 5841−5866.

(17) Nakamura, Y.; Aratani, N.; Osuka, A. Cyclic porphyrin arrays as artificial photosynthetic antenna: Synthesis and excitation energy transfer. *Chem. Soc. Rev.* **2007**, *36*, 831−845.

(18) Bogaerts, T.; Van Yperen-De Deyne, A.; Liu, Y. Y.; Lynen, F.; Van Speybroeck, V.; Van Der Voort, P. Mn-salen@MIL101(Al): a heterogeneous, enantioselective catalyst synthesized using a 'bottle around the ship' approach. *Chem. Commun.* **2013**, *49*, 8021−8023.

(19) Shultz, A. M.; Farha, O. K.; Hupp, J. T.; Nguyen, S. T. A catalytically active, permanently microporous MOF with metalloporphyrin struts. *J. Am. Chem. Soc.* **2009**, *131*, 4204−4205.

(20) Krishna Kumar, R.; Goldberg, I. Crystal engineering with tetraarylporphyrins, an exceptionally versatile building block for the design of multidimensional supramolecular structures. *Chem. Commun.* **1998**, 1435−1436.

(21) Feng, D. W.; Gu, Z. Y.; Li, J. R.; Jiang, H. L.; Wei, Z. W.; Zhou, H. C. Zirconium-metalloporphyrin PCN-222: mesoporous metal-organic frameworks with ultrahigh stability as biomimetic Catalysts. *Angew. Chem., Int. Ed.* **2012**, *51*, 10307−10310.

(22) Song, F. J.; Wang, C.; Falkowski, J. M.; Ma, L. Q.; Lin, W. B. Isoreticular chiral metal-organic frameworks for asymmetric alkene epoxidation: tuning catalytic activity by controlling framework catenation and varying open channel sizes. *J. Am. Chem. Soc.* **2010**, *132*, 15390−15398.

(23) Kosal, M. E.; Chou, J. H.; Wilson, S. R.; Suslick, K. S. A functional zeolite analogue assembled from metalloporphyrins. *Nat. Mater.* **2002**, *1*, 118−121.
(24) Peng, R.; Li, M.; Li, D. Copper(I) halides: A versatile family in coordination chemistry and crystal engineering. *Coord. Chem. Rev.* **2010**, *254*, 1−18.
(25) Hou, Y. L.; Sun, R. W. Y.; Zhou, X. P.; Wang, J. H.; Li, D. A copper(I)/copper(II)-salen coordination polymer as a bimetallic catalyst for three-component Strecker reactions and degradation of organic dyes. *Chem. Commun.* **2014**, *50*, 2295−2297.
(26) Hou, Y. L.; Pi, Y.; Zhou, X. P.; Li, D. An in situ embedded square-planar $Cu^{II}/Ni^{II}N_4$ metalloligand in coordination polymers for visible-light photocatalysis. *Inorg. Chem.* **2018**, *57*, 2377−2380.
(27) Hu, Z.; Deibert, B. J.; Li, J. Luminescent metal-organic frameworks for chemical sensing and explosive detection. *Chem. Soc. Rev.* **2014**, *43*, 5815−5840.
(28) Drummond, M. L.; Cundari, T. R.; Wilson, A. K. Cooperative carbon capture capabilities in multivariate MOFs decorated with amino acid side chains: a computational study. *J. Phys. Chem. C* **2013**, *117*, 14717−14722.
(29) Huang, Y.-B.; Liang, J.; Wang, X.-S.; Cao, R. Multifunctional metal−organic framework catalysts: synergistic catalysis and tandem reactions. *Chem. Soc. Rev.* **2017**, *46*, 126−157.
(30) Easun, T. L.; Moreau, F.; Yan, Y.; Yang, S.; Schröder, M. Structural and dynamic studies of substrate binding in porous metal−organic frameworks. *Chem. Soc. Rev.* **2017**, *46*, 239−274.
(31) Lin, Z.-J.; Lü, J.; Hong, M.; Cao, R. Metal−organic frameworks based on flexible ligands (FL-MOFs): structures and applications. *Chem. Soc. Rev.* **2014**, *43*, 5867−5895.
(32) Liao, L.; Ingram, C. W.; Bacsa, J.; Zhang, Z. J.; Dinadayalane, T. A hydrogen bonded Co(ii) coordination complex and a triply interpenetrating 3-D manganese(ii) coordination polymer from diaza crown ether with dibenzoate sidearms. *CrystEngComm* **2016**, *18*, 2425−2436.
(33) Schneemann, A.; Bloch, E. D.; Henke, S.; Llewellyn, P. L.; Long, J. R.; Fischer, R. A. Influence of solvent-like sidechains on the adsorption of light hydrocarbons in metal-organic frameworks. *Chem. - Eur. J.* **2015**, *21*, 18764−18769.
(34) Cui, J.; Wong, Y.-L.; Zeller, M.; Hunter, A. D.; Xu, Z. Pd uptake and H_2S sensing by an amphoteric metal-organic framework with a soft core and rigid side arms. *Angew. Chem., Int. Ed.* **2014**, *53*, 14438−14442.
(35) Bobbitt, N. S.; Mendonca, M. L.; Howarth, A. J.; Islamoglu, T.; Hupp, J. T.; Farha, O. K.; Snurr, R. Q. Metal−organic frameworks for the removal of toxic industrial chemicals and chemical warfare agents. *Chem. Soc. Rev.* **2017**, *46*, 3357−3385.
(36) Wang, P.-L.; Xie, L.-H.; Joseph, E. A.; Li, J.-R.; Su, X.-O.; Zhou, H.-C. Metal−organic frameworks for food safety. *Chem. Rev.* **2019**, *119*, 10638−10690.
(37) He, J.; Zha, M.; Cui, J.; Zeller, M.; Hunter, A. D.; Yiu, S.-M.; Lee, S.-T.; Xu, Z. Convenient detection of Pd(II) by a metal−organic framework with sulfur and olefin Functions. *J. Am. Chem. Soc.* **2013**, *135*, 7807−7810.
(38) Wang, A.; Hou, Y.-L.; Kang, F.; Lyu, F.; Xiong, Y.; Chen, W.-C.; Lee, C.-S.; Xu, Z.; Rogach, A. L.; Lu, J.; Li, Y. Y. Rare earth-free composites of carbon dots/metal−organic frameworks as white light emitting phosphors. *J. Mater. Chem. C* **2019**, *7*, 2207−2211.
(39) Hou, Y.-L.; Li, M.-Q.; Cheng, S.; Diao, Y.; Vilela, F.; He, Y.; He, J.; Xu, Z. Dramatic improvement of stability and electroactivity by linker cyclization of a metal-organic framework. *Chem. Commun.* **2018**, *54*, 9470−9473.
(40) Ji, Q.; Li, L.; Deng, S.; Cao, X.; Chen, L. High switchable dielectric phase transition originating from distortion in inorganic−organic hybrid materials (H_2dabco-C_2H_5) [$M^{II}Cl_4$] (M = Co, Zn). *Dalton Trans.* **2018**, *47*, 5630−5638.
(41) Chen, L.; Ji, Q.; Wang, X.; Pan, Q.; Cao, X.; Xu, G. Two novel metal−organic coordination polymers based on ligand 1,4-diazabicyclo[2.2.2]octane N, N′-dioxide with phase transition, and ferroelectric and dielectric properties. *CrystEngComm* **2017**, *19*, 5907−5914.
(42) Chen, L.-Z.; Huang, D.-D.; Ge, J.-Z.; Wang, F.-M. Temperature-induced reversible structural phase transition of 1-(chloromethyl)-1,4-diazoniabicyclo[2.2.2]octane bis(perchlorate). *CrystEngComm* **2014**, *16*, 2944−2949.
(43) Chen, L.-Z.; Huang, D.-D.; Ge, J.-Z.; Pan, Q.-J. Reversible ferroelastic phase transition of N-chloromethyl-1,4-diazabicyclo-[2.2.2]octonium trichlorobromoaquo copper(II). *Inorg. Chem. Commun.* **2014**, *45*, 5−9.
(44) Chen, L.-Z.; Huang, D.-D.; Pan, Q.-J.; Ge, J.-Z. Novel pure Pnma−P212121 ferroelastic phase transition of 1,4-diisopropyl-1,4-diazonia-bicyclo[2.2.2]octane tetra-chlorobromo-M(II) (M1/4Mn and Co). *RSC Adv.* **2015**, *5*, 13488−13494.
(45) Qian, X.; Deng, S.; Chen, X.; Gao, Q.; Hou, Y.-L.; Wang, A.; Chen, L. A highly stable, luminescent and layered zinc(II)-MOF: iron(III)/copper(II) dual sensing and guest-assisted exfoliation. *Chin. Chem. Lett.* **2019**, DOI: 10.1016/j.cclet.2019.09.024.
(46) Hu, F.-L.; Mi, Y.; Zhu, C.; Abrahams, B. F.; Braunstein, P.; Lang, J.-P. Stereoselective solid-state synthesis of substituted cyclobutanes assisted by pseudorotaxane-like MOFs. *Angew. Chem., Int. Ed.* **2018**, *57*, 12696−12701.
(47) Chen, Q.-F.; Zhao, X.; Liu, Q.; Jia, J.-D.; Qiu, X.-T.; Song, Y.-L.; Young, D. J.; Zhang, W.-H.; Lang, J.-P. Tungsten(VI)−copper(I)−sulfur cluster-supported metal−organic frameworks bridged by in situ click-formed tetrazolate ligands. *Inorg. Chem.* **2017**, *56*, 5669−5679.
(48) Chen, X.; Li, H.-X.; Zhang, Z.-Y.; Zhao, W.; Lang, J.-P.; Abrahams, B. F. Activation and amplification of the third-order NLO and luminescent responses of a precursor cluster by a supramolecular approach. *Chem. Commun.* **2012**, *48*, 4480−4482.
(49) Liu, Q.; Zhang, W.-H.; Lang, J.-P. Versatile thiomolybdate-(thiotungstate)−copper−sulfide clusters and multidimensional polymers linked by cyanides. *Coord. Chem. Rev.* **2017**, *350*, 248−274.
(50) Zhang, W.-H.; Ren, Z.-G.; Lang, J.-P. Rational construction of functional molybdenum (tungsten)−copper−sulfur coordination oligomers and polymers from preformed cluster precursors. *Chem. Soc. Rev.* **2016**, *45*, 4995−5019.
(51) Chen, L.; Li, H.-X.; Dai, M.; Li, H.-Y.; Lang, J.-P. Capturing the organic species derived from the C−C cleavage and in situ oxidation of 1,2,3,4-tetra(pyridin-4-yl)cyclobutane by [CuCN]n-based MOFs. *Inorg. Chem.* **2018**, *57*, 9160−9166.
(52) Peng, Y.-L.; Liu, J.; Zhang, H.-F.; Luo, D.; Li, D. A size-matched POM@MOF composite catalyst for highly efficient and recyclable ultra-deep oxidative fuel desulfurization. *Inorg. Chem. Front.* **2018**, *5*, 1563−1569.
(53) Du, J.-J.; Zhang, X.; Zhou, X.-P.; Li, D. Robust heterometallic MOF catalysts for the cyanosilylation of aldehydes. *Inorg. Chem. Front.* **2018**, *5*, 2772−2776.
(54) Li, Y.; He, T.-Y.; Dai, R.-R.; Huang, Y.-L.; Zhou, X.-P.; Chen, T.; Li, D. Bifunctional gyroidal MOFs: highly efficient lewis base and lewis acid catalysts. *Chem. - Asian J.* **2019**, *14*, 3682−3687.

https://dx.doi.org/10.1021/acs.cgd.9b01499
Cryst. Growth Des. 2020, 20, 1237−1241